ACS APPLIED MATERIALS & INTERFACES

Research Article

www.acsami.org

Multifunctional Chitosan-45S5 Bioactive Glass-Poly(3-hydroxybutyrate-*co*-3-hydroxyvalerate) Microsphere Composite Membranes for Guided Tissue/Bone Regeneration

Wei Li,[†] Yaping Ding,[‡] Shanshan Yu,[§] Qingqing Yao,*[,§] and Aldo R. Boccaccini*[,†]

[†]Institute of Biomaterials, Department of Materials Science and Engineering, University of Erlangen-Nuremberg, Cauerstrasse 6, 91058 Erlangen, Germany

[‡]Institute of Polymer Materials, Department of Materials Science and Engineering, University of Erlangen-Nuremberg, Martensstrasse 7, 91058 Erlangen, Germany

[§]Institute of Advanced Materials for Nano-Bio Applications, School of Ophthalmology and Optometry, Wenzhou Medical University, 270 Xueyuan Xi Road, Wenzhou, Zhejiang 325027, China

Supporting Information

ABSTRACT: Novel multifunctional chitosan-45S5 bioactive glass-poly(3-hydroxybutyrate-*co*-3-hydroxyvalerate) (PHBV) microsphere (CS-BG-MS) composite membranes were developed with applicability in guided tissue/bone regeneration (GTR/GBR). The incorporation of 45S5 BG and PHBV MS into CS membranes not only provided the membranes with favorable surface roughness, hydrophilicity, and flexibility but also slowed down their degradation rate. Moreover, the CS membranes became bioactive after the incorporation of 45S5 BG and capable of releasing drugs of different physicochemical properties in a controlled and sustained manner with the addition of PHBV MS. Cell culture tests showed that osteoblast-like MG-63 human osteosarcoma cells had significantly higher adhesion, cell proliferation, and alkaline phosphatase (ALP) activity on CS-BG and CS-BG-MS membranes than on neat CS membranes. Therefore, the developed bioactive CS-BG-MS membranes with potential multidrug (e.g., antibacterial and antiosteoporosis drugs) delivery capability are promising candidate membranes for GTR/GBR applications.

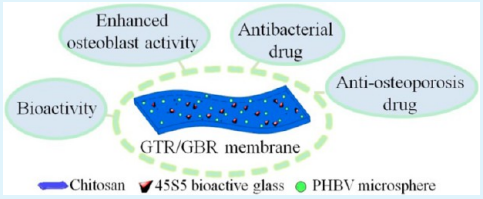

KEYWORDS: *chitosan, 45S5 bioactive glass, PHBV microsphere, drug delivery, membrane, guided bone regeneration*

1. INTRODUCTION

Periodontitis is a set of inflammatory diseases of the periodontal tissues. Periodontal regeneration is necessary when the bone supporting the teeth has been lost to periodontitis, which is however challenging due to the complexity of the biological events, factors, and cells underlying the healing process.[1] Ideal treatment strategies should be able to regenerate all lost periodontal tissues, including the gingiva, periodontal ligament (PDL), cementum, and alveolar bone.[2,3] Periodontal regeneration has been achieved following the principle of guided tissue regeneration (GTR).[1] The GTR process typically involves application of a barrier membrane to prevent fast migrating epithelial cells as well as gingival tissues from reaching the defect sites, allowing the necessary time for the formation of PDL, cementum, and bone.[2,4] Moreover, barrier membranes have also been used in the regeneration of bone surrounding peri-implant defects, which is defined as guided bone regeneration (GBR).[3,5] Membranes used in GTR/GBR are divided into resorbable and nonresorbable membranes. There is increasing interest in the use of resorbable membranes owing to the suppression of a second surgical procedure for membrane removal.[6]

Resorbable collagen has been widely used to produce GTR/GBR membranes, which however presents some disadvantages such as fast *in vivo* degradation, poor mechanical strength, and risk of disease transmission.[3] In order to avoid these undesirable features, a wide variety of alternative polymers has been proposed.[3,6−8] Chitosan (CS), an alkaline polysaccharide obtained from the deacetylation of chitin, has been shown to be an attractive candidate material for GTR/GBR membranes due to its low cost, superior biocompatibility, nonantigenicity, appropriate degradation rate, flexibility in hydrated environments, and hemostatic activity.[2,5,9]

It should be pointed out that, to date, the regeneration potential of periodontal tissues using current polymer membranes including chitosan is usually limited to restore only a fraction of the original tissue volume, although statistical significance was achieved.[5] GTR/GBR membranes capable of promoting faster bone growth as well as releasing relevant therapeutic drugs are suggested to be highly effective for periodontal regeneration.[3] It has been shown in previous studies that the incorporation of bioactive glasses/ceramics can significantly enhance mineralization and cell activities on polymer membranes, indicating favorable osteoconductivity

Received: July 8, 2015
Accepted: August 28, 2015
Published: August 28, 2015

DOI: 10.1021/acsami.5b06128
ACS Appl. Mater. Interfaces 2015, 7, 20845−20854

and/or osteoinductivity for GTR/GBR applications.[2,4,7,10] Among the available bioactive glasses/ceramics, 45S5 bioactive glass (BG) has received increasing attention in bone regeneration owing to its excellent bioactivity, biocompatibility, and osteogenic and potential angiogenic effects.[11−13] Moreover, the ability of 45S5 BG to regenerate not only hard tissues but also soft tissues is of particular interest in periodontal regeneration because the periodontal tissues consist of both hard tissues (i.e., cementum and alveolar bone) and soft tissues (i.e., gingiva and PDL).[14]

The development of periodontitis is mainly related to bacteria activities.[3,15] Moreover, bacterial infections are currently considered to be the major reason for the failure of GTR/GBR membranes in clinical applications.[8] Therefore, antibiotics are frequently used to prevent/treat bacterial infections in periodontal defects in order to aid periodontal regeneration.[3] GTR/GBR membranes loaded with antibiotics have been designed for local drug release in order to overcome the adverse effects of conventional systemic drug administration.[3,5,8] Since antibiotics were generally directly blended with the matrix of GTR/GBR membranes, the drugs were rapidly released from the membranes, resulting in a high burst release and short release period that could not effectively prevent bacterial infections. Hence, there is a strong demand to develop novel sustained and controlled drug delivery systems for GTR/GBR applications. Polymer microspheres are well-known for their ability to encapsulate a wide range of drugs and to provide sustained and controlled drug release profiles.[16] For example, poly(3-hydroxybutyrate-*co*-3-hydroxyvalerate) (PHBV) microspheres can release vancomycin in a lower burst release and for a much longer release period than the continuous PHBV film/layer as shown in our previous studies.[17,18] PHBV is a copolymer of PHB and PHV and has been used for preparing microspheres for drug delivery purposes due to its good biocompatibility and tailorable degradability.[17,19] Moreover, during the degradation process, PHBV does not produce acidic degradation products (like PLA or PLGA) which may be harmful for human tissues.[20] These advantages make PHBV microspheres also attractive as drug carriers for GTR/GBR applications.

Osteoporosis, which is characterized by a significant decrease in bone mass, has been found to significantly increase the risk of developing periodontitis, especially in postmenopausal women.[21−23] The presence of insufficient bone mass such as alveolar bone may delay the healing of periodontal defects due to reduced bone remodeling. Therefore, it would be necessary to endow the GTR/GBR membranes with antiosteoporosis drug release function in order to enhance the periodontal regeneration in osteoporosis patients, whose number continues to grow due to the increasing aging population.[24]

In the present study, PHBV microspheres were embedded into CS matrix to serve as drug carriers aiming to release antibiotics and antiosteoporosis drugs in a controlled and sustained manner, and the CS membranes were expected to be bioactive after the incorporation of 45S5 BG. Chitosan (CS), chitosan-45S5 BG (CS-BG), and chitosan-45S5 BG-PHBV microsphere (CS-BG-MS) membranes were prepared through the solution casting method, and the morphology, physicochemical properties, *in vitro* bioactivity, and cell response of these membranes were studied. The cell biology evaluation was carried out using osteoblast-like MG-63 human osteosarcoma cells. In order to demonstrate the drug delivery capability and to investigate the drug release behavior, tetracycline hydrochloride (TCH) and daidzein were chosen as model drugs for antibacterial and antiosteoporosis purposes in the present study, respectively. TCH is a broad-spectrum antibiotic, with activity against both Gram-positive and Gram-negative bacteria. Daidzein is one of the main isoflavones abundant in soybean and pueraria and shows an antiosteoporosis effect.[25] In addition, TCH and daidzein were chosen also because they could serve as typical hydrophilic and hydrophobic model drugs, respectively.

2. MATERIALS AND METHODS

2.1. Materials. CS from shrimp shells (low viscosity) was purchased from Sigma-Aldrich (St. Louis, MO, USA). Commercially available melt-derived 45S5 BG powder of particle size ∼2 μm was used. PHBV (PHV 12 wt %) was obtained from Goodfellow (Huntingdon, UK). TCH and daidzein were purchased from AppliChem (Darmstadt, Germany) and Cayman Chemicals (Ann Arbor, MI, USA), respectively. Poly(vinyl alcohol) (PVA) (MW ∼ 30 000) was supplied by Merck (Darmstadt, Germany). All the other chemicals for microsphere, simulated body fluid (SBF) and phosphate buffered saline (PBS) preparation were purchased from Sigma-Aldrich (St. Louis, MO, USA).

2.2. PHBV Microsphere Preparation. The double emulsion solvent evaporation method was used to prepare TCH loaded PHBV microspheres.[17] 4.5 mg of TCH was dissolved in 0.15 mL of 2% w/v aqueous PVA solution. This solution was then added into 3 mL of 3% w/v PHBV−dichloromethane solution. The mixture was emulsified using a probe sonicator (Branson Sonifier S-250D, Emerson, USA) at 20% power output for 40 s. The resultant primary emulsion was immediately added into 75 mL of 2% w/v aqueous PVA solution and emulsified using a homogenizer (T18, IKA, Germany) at 7000 rpm for 3 min. The resultant double emulsion was then stirred at 600 rpm for 2 h. The microspheres were collected by centrifugation (Centrifuge 5430R, Eppendorf, Germany), washed 3 times in deionized water, and freeze-dried (Alpha 1-2 LD plus, Martin Christ, Germany). Daidzein loaded microspheres were prepared by the single emulsion method modified from the aforementioned double emulsion method. The only difference was that daidzein was directly added into PHBV solution without the aid of a primary emulsion process.

2.3. Fabrication of Membranes. The membranes were obtained by the solution casting method. 0.7 g of CS was dissolved in 35 mL of aqueous acetic acid solution (1% v/v) to a concentration of 2% w/v. For pure CS membranes, 35 mL of ethanol was added to the above CS solution. For CS-BG membranes, 0.175 g of 45S5 BG was dispersed in 35 mL of ethanol and then added to the CS solution, while for CS-BG-MS membranes, 0.2 g of 45S5 BG and 0.1 g of MS were dispersed together in 35 mL of ethanol before being added to the CS solution. After homogenization for 10 min, the CS, CS-BG, and CS-BG-MS solutions were cast onto ⌀ 7 cm × 1 cm Teflon Petri dishes and then left to dry at room temperature for 3 days.

2.4. Physicochemical Characterization. *2.4.1. Surface Morphology.* The microstructure and surface morphology of the membranes were studied using scanning electron microscopy (SEM) (LEO 435 VP, Cambridge, UK and Ultra Plus, Zeiss, Germany). Samples were gold-sputtered before observation.

2.4.2. Elemental Analysis. The elemental analysis of the samples was carried out using energy dispersive spectroscopy (EDS, X-Max^N Oxford Instruments, UK). The EDS analysis was performed at 8 kV and a working distance of 6 mm. Samples were carbon-sputtered before EDS analysis.

2.4.3. Roughness Measurement. The roughness measurements of the membranes were carried out using a laser profilometer (UBM). A reflection of 670 nm laser beam was used to determine the vertical position of the membrane surface. The roughness was measured on the top surface and represented as average roughness (R_a), maximum peak-to-valley height (R_{max}), and mean peak-to-valley height (R_{zDIN}).

2.4.4. Contact Angle Measurement. The static contact angle on membranes was determined by a DSA30 contact angle measuring instrument (Kruess, Germany). Water with a volume of 3 μL was

DOI: 10.1021/acsami.5b06128
ACS Appl. Mater. Interfaces 2015, 7, 20845−20854

added on the samples by a motor-driven syringe. The results were reported by averaging the results of five measurements.

2.4.5. Tensile Testing. The characterization of mechanical strength was performed using a standard tensile strength test (Frank, Karl Frank GmbH, Germany) on 5 mm × 40 mm strips of ∼100 μm thickness with a gauge length of 20 mm and a load cell capacity of 50 N under a loading speed of 10 mm/min. The ultimate tensile strength, elongation at break, and Young's modulus were determined from the stress−strain curves. Work of fracture was also calculated. Five samples were tested for each composition.

2.4.6. In Vitro Bioactivity Test. The *in vitro* bioactivity of CS-BG and CS-BG-MS membranes was performed in SBF.[26] The membranes with dimensions of 5 mm × 10 mm × ∼100 μm were immersed in 50 mL of SBF and maintained at 37 °C in a shaking incubator (90 rpm) for 1, 3, 7, and 14 days. The SBF was replaced twice per week. After each given time interval, the membranes were removed from the incubator, rinsed with deionized water, and left to dry at room temperature for further analysis. For FTIR (Nicolet 6700, Thermo Scientific, USA), the membranes were cut, ground, mixed with KBr (spectroscopy grade, Merck, Germany), and pressed into pellets. XRD and SEM were performed directly on membranes.

2.4.7. Swelling and Degradation. The swelling and degradation behaviors of CS, CS-BG, and CS-BG-MS membranes were studied together with the bioactivity test. Samples were dried before the experiment. After immersion in SBF for different periods of time, wet membranes were wiped with filter paper to remove excess liquid and weighed. The swelling ratio was calculated by eq 1:

$$\text{swelling ratio}\,(\%) = (M_2 - M_1)/M_1 \times 100\% \quad (1)$$

where M_1 and M_2 are the mass of the samples before and after swelling, respectively.

After drying the wet membranes, they were weighed again and the weight loss was calculated by eq 2:

$$\text{weight loss}\,(\%) = (M_1 - M_3)/M_1 \times 100\% \quad (2)$$

where M_3 is the mass of the samples after drying. For each time point, three samples were measured.

2.5. Drug Release. *2.5.1. Drug Release Test.* The drug release behavior of MS, CS membranes, and CS-BG-MS membranes was studied. For CS-BG-MS membranes, TCH or daidzein was incorporated by using TCH or daidzein loaded MS. For CS membranes, TCH or daidzein was incorporated by adding TCH or daidzein into the CS solution at a mass ratio of 1:200 during the membrane preparation. 50 mg/10 mg MS, 250 mg/50 mg CS, and 500 mg/100 mg CS-BG-MS membranes were placed in a dialysis bag (Spectra/Por 1, molecular weight cutoff 6000 to 8000, Carl Roth, Germany) for the TCH/daidzein release study, respectively, and then immersed in centrifuge tubes containing 10 mL of release medium. PBS solution (pH 7.4) was used for the TCH release study, while a mixture solution consisting of 75 vol % PBS and 25 vol % ethanol was used for the daidzein release study in order to meet sink conditions.[27] The samples were incubated in a shaking incubator (90 rpm, 37 °C). At predetermined time intervals, 1 mL of medium from each sample was extracted and the medium was replenished with 1 mL of fresh release medium. The amount of TCH and daidzein was measured using the UV−Vis spectrophotometer (Specord 40, Analytik Jena, Germany) at wavelengths of 362 and 252 nm, respectively.

2.5.2. Drug Release Kinetics. Higuchi and Peppas models, as represented by eqs 3 and 4, were used to analyze the drug release kinetics.[28,29]

$$Q_t = kt^{1/2} \quad (3)$$

$$Q_t = kt^n \quad (4)$$

where Q_t is the cumulative percentage drug release, k is the kinetic constant, n is the release exponent which defines the mechanism of drug release, and t is the release time. These equations are generally valid for the first 60% of total amount of drug release.

2.6. Cell Biology Study. The human osteosarcoma cell line (MG-63) was purchased from American Type Culture Collection (ATCC, USA) and were cultured in a Dulbecco's modification of Eagle's medium (Gibco, Invitrogen, USA), containing 10% fetal bovine serum (Gibco, Invitrogen, USA) and 6 μg/mL gentamicin (Gibco, Invitrogen, USA). Cells were cultured under a humidified atmosphere with 5% CO_2 at 37 °C. The medium was changed every 2 or 3 days.

2.6.1. Sample Preparation. The CS, CS-BG, and CS-BG-MS membranes for the cell biology study were prepared by casting the corresponding solution prepared in Section 2.3 into well plates. In order to obtain membranes with the same thickness, 0.554 and 0.078 mL solutions were added into each well of the 24-well plates and 96-well plates, respectively. The samples were left to dry at room temperature for 3 days and then sterilized under UV light for 2 h.

2.6.2. Cell Viability. Cell viability was quantitatively analyzed using Cell Counting Kit-8 (CCK8, Dojindo, Japan). Cells were seeded into 96-well plates at 2000 cells/well and incubated for 1 and 2 days. The absorbance of produced WST-8 formazan at 450 nm was measured by a microplate reader (Model 680, Bio-Rad Laboratories, USA). All results were demonstrated as optical density (OD) values minus the absorbance of blank wells.

2.6.3. Live/Dead Assay. For Live/Dead staining, 1×10^5 cells were seeded into each well of 24-well plates and cultured for 1 and 4 days. The samples were subsequently washed with PBS solution for 3 times. Cells were labeled with a freshly made solution of dyes taken from a final concentration of 10 μM calcein AM and 15 μM PI in PBS. After staining for 15 min at 37 °C, the samples were washed with PBS for 3 times and observed with a fluorescence microscope (IX 2-UCB, Olympus, Germany).

2.6.4. Cell Skeleton and Morphology. The cytoskeleton organization of MG-63 cells grown on the extracts of the CS, CS-BG, and CS-BG-MS membranes was analyzed using Filamentous actin (F-actin) staining. The sterilized samples (1×1 cm^2) were placed into a 24-well flat culture plate, and a 1×1 cm^2 glass coverslip was then located on the top completely covering the surface of each sample; after that, 1×10^4 cells/mL were seeded into each well and cultured for 1 and 4 days, respectively. Cells were subsequently fixed with 4% paraformaldehyde for 10 min, permeabilized with 0.1% TritonX-100 for 5 min, blocked with 1% bovine serum albumin for 20 min, stained with Rhodamine Phalloidin for 20 min, and stained with DAPI for 5 min in the dark. The stained MG-63 cells were observed under laser scanning microscopy (LSM 710, Zeiss, Germany).

For cell morphology characterization, samples were immersed in DMEM for 4 h in a cell incubator, and then, 4×10^4 MG-63 cells were seeded into each well and cultured for 1 day. After cultivation, the samples were washed twice with PBS solution and fixed in 2.5% glutaraldehyde for 3 h at 4 °C. The samples were subsequently dehydrated in ethanol solutions of various concentrations (30, 50, 70, 90, and 100 vol %) for 15 min, respectively, prior to being freeze-dried. After being completely dried, the morphology of the cells was observed by SEM (Nova NanoSEM, FEI).

2.6.5. Alkaline Phosphatase Activity. Alkaline phosphatase (ALP) activity was measured using an ALP assay kit (Beyondtime Bio-Tech, China). 5×10^3 MG-63 cells were seeded into membranes in 24-well plates and cultured for 7 and 14 days. At every specific time point, samples were rinsed with PBS solution and lysed with 0.1% Trion X-100 solution for 30 min at 4 °C; the solution was then transferred into a tube and centrifuged at 3000 rpm for 2 min at 4 °C. 50 μL of the prepared supernatant of each sample was mixed with 50 μL of chromogenic substrate (para-Nitrophenylphosphate) and cultured for 10 min at 37 °C. Following the incubation, the reaction was stopped by adding 100 μL of terminated liquid. ALP activity was measured at 405 nm using a microplate reader.

2.6.6. Statistical Analysis. Statistical differences were determined by SPSS 16.0. All results were expressed as the mean ± standard deviation. $P < 0.05$ was considered as being statistically significant.

DOI: 10.1021/acsami.5b06128
ACS Appl. Mater. Interfaces 2015, 7, 20845−20854

3. RESULTS AND DISCUSSION

3.1. Surface Morphology. The shape and surface morphology of the prepared TCH and daidzein loaded MS are shown in Figure 1, showing the well formed spherical shape.

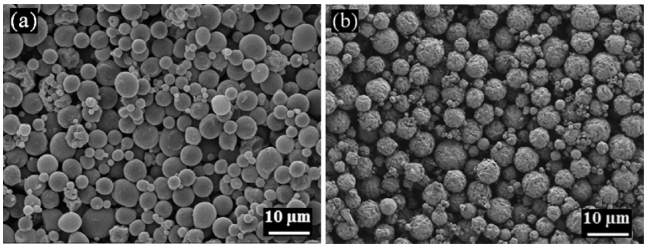

Figure 1. SEM images of PHBV microspheres loaded with (a) TCH and (b) daidzein.

Daidzein loaded MS presented a relatively rougher surface than TCH loaded MS, which may be caused by the different hydrophilicity of the drugs. According to our previous study on PHBV microspheres using similar preparation parameters, 50% of the MS had diameters below 3.5 μm and 90% of the MS below 7 μm.[17]

The surface morphology of the prepared membranes is shown in Figure 2a–c. The pure CS membranes presented a

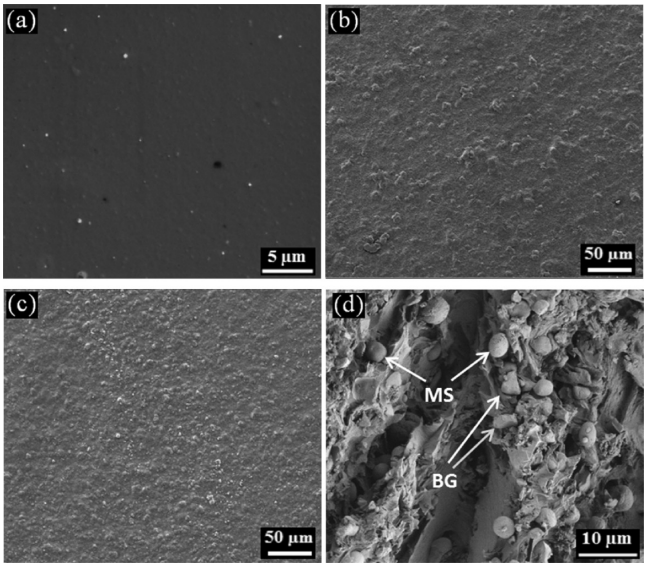

Figure 2. SEM images of (a) CS membranes, (b) CS-BG membranes, (c) CS-BG-MS membranes, and (d) cross-section of CS-BG-MS membranes, in which the arrows indicate the presence of MS and BG.

flat and smooth surface (Figure 2a). The few visible particles on pure CS membranes may be the result of impurities deposited on the surfaces during the drying process. CS-BG and CS-BG-MS membranes (Figure 2b,c) showed a relatively rougher surface in comparison to the CS membranes, and some asperities were seen homogeneously distributed on the surfaces corresponding to BG and MS. Figure 2d shows the cross-section of a typical CS-BG-MS membrane, where spherical MS and irregular BG particles were found to be fairly homogeneously dispersed in the CS matrix. The homogeneous distribution of BG particles on the surface and in the cross-section of the CS-BG-MS membrane was further confirmed by EDS mapping (Figures S1 and S2).

3.2. Surface Roughness. The surface roughness of the membranes is shown in Table 1. An increase of roughness (R_a) in the submicroscale was obtained after the addition of BG, and the roughness was further increased after the addition of MS. Compared to the particle size of BG and MS, the R_a did not increase to a large extent. This is likely due to the fact that most of the BG and MS were embedded inside rather than on top of the membranes. The significant increase of R_{max} and R_{zDIN} in the microscale is probably mainly due to the existing few agglomerated BG and MS in the membranes (Figure 2b,c). It has been shown on PCL discs with hydroxyapatite (HA) coatings that surfaces with increased submicro- and microscale complexity and roughness can significantly enhance osteoblast attachment and expression of osteogenic markers.[30]

Table 1. Surface Roughness Parameters of CS, CS-BG, and CS-BG-MS Membranes

	roughness (μm)		
sample	R_a	R_{max}	R_{zDIN}
CS	0.20 ± 0.02	3.1 ± 0.3	2.0 ± 0.2
CS-BG	0.40 ± 0.09	6 ± 2	5 ± 1
CS-BG-MS	0.7 ± 0.2	10 ± 3	7 ± 2

3.3. Mechanical Properties. Table 2 summarizes the tensile strength, elongation at break, work of fracture, and Young's modulus of CS, CS-BG, and CS-BG-MS membranes, and Figure S3 displays representative stress–strain curves. As shown in Figure S3, the fracture behavior of CS-BG-MS membranes turned into ductile fracture despite the brittle character of the pure CS membranes, which indicates the great enhancement of toughness due to the incorporation of BG and MS. The increase of elongation at break and work of fracture quantitatively confirmed the toughening effect of BG and MS (Table 2). The toughening effect could be attributed to crack pinning and crack deflection mechanisms, introduced by the incorporated rigid BG and MS particles, which resulted in the limitation of the propagation of cracks during tensile loading, leading to the enhancement of toughness and elongation at break.[31] However, the tensile strength and Young's modulus of the membranes decreased 41% and 39%, respectively, owing to the BG and MS addition, which may be caused by stress concentrations in the matrix that result from mismatch of the Young's modulus between the added particles (BG and MS) and the CS matrix. Similar behavior has been observed in other studies about polymers filled with particles.[31] Overall, the membranes were less strong but more flexible than pure CS after the addition of BG and MS, and these properties may ensure easy handling and cutting of membranes while performing a surgical procedure.

Table 2. Mechanical Properties of CS, CS-BG, and CS-BG-MS Membranes

sample	tensile strength (MPa)	elongation at break (%)	work of fracture (J)	Young's modulus (GPa)
CS	43 ± 2	8.0 ± 0.6	5.4 ± 0.5	0.83 ± 0.02
CS-BG	38 ± 1	10 ± 1	7.2 ± 0.5	0.72 ± 0.07
CS-BG-MS	25 ± 2	16 ± 4	10 ± 1	0.51 ± 0.07

3.4. Contact Angle. The hydrophilicity of the prepared membranes, which may significantly influence cell activity,[32,33]

DOI: 10.1021/acsami.5b06128
ACS Appl. Mater. Interfaces 2015, 7, 20845–20854

was measured by determining the contact angle with water. The contact angle of the CS membranes considerably decreased with the addition of hydrophilic BG and further decreased after the incorporation of MS (Table 3). The contact angle of PHBV films was reported to be 100° ± 4°,[18] indicating a potential hydrophobic characteristic of PHBV microspheres, while the contact angle of the CS-BG-MS membranes was lower than that of the CS-BG membranes. It is well-known that both topographic features and surface chemistry could influence the surface hydrophilicity of materials.[34] The decrease of contact angle in the CS-BG-MS membranes may be due to their rougher surface compared to the CS-BG membranes, as indicated in Table 1.

Table 3. Water Contact Angle Values of CS, CS-BG, and CS-BG-MS Membranes

sample	CS membranes	CS-BG membranes	CS-BG-MS membranes
contact angle (deg)	103 ± 5	78 ± 6	63 ± 4

3.5. *In Vitro* Bioactivity Test. The *in vitro* bioactivity of the membranes was analyzed by assessing their ability to induce the formation of HA upon immersion in SBF. Figure 3 shows the XRD spectra of the CS-BG-MS membranes before and after immersion in SBF. HA peaks were found after 1 day of immersion, and their intensity increased with the extension of immersion time. FTIR spectra of the CS-BG and CS-BG-MS membranes before and after immersion in SBF are presented in Figure 4. Before immersion, CS-BG and CS-BG-MS membranes presented the characteristic bands of PHBV at 1726 cm^{-1}, due to the C═O stretching vibrational bands. The bands at around 1560 cm^{-1} can be assigned to the stretching vibration of amide II in CS, while the bands at around 1650 cm^{-1} are due to the stretching vibration of amide I. After immersion for different times, CS-BG and CS-BG-MS membranes exhibited P−O bands at around 567 and 603 cm^{-1}, which is characteristic of a crystalline phosphate phase.[35] The formation of the bands at around 897 cm^{-1} and the dual broad band between 1420 and 1480 cm^{-1} are attributed to the stretching and bending vibrations of C−O bond, respectively, suggesting the formed HA is HCA rather than stoichiometric HA.[35,36] Furthermore, the characteristic band of CS at around 1565 cm^{-1} shifted to 1595 cm^{-1}, implying that inter hydrogen bonds existed between CS and HCA.[37,38] Surface morphologies of the CS-BG and CS-BG-MS membranes after 7 days of immersion in SBF were observed by SEM (Figure 5). Apatite-like layer was more visible on the surface of CS-BG-MS membranes than on CS-BG membranes. EDS analysis was performed to detect the nature of the formed apatite-like layer by evaluating the Ca/P ratio, and the results for CS-BG-MS membranes (Figure S4) showed that the Ca/P molar ratio was 1.47 ± 0.06, indicating a nonstoichiometric HA layer.

All results presented above demonstrated that HCA began to form on the CS-BG-MS membranes after 1 day of immersion in SBF confirming that the presence of MS did not inhibit the bioactivity that 45S5 BG endowed to the CS-BG membranes.

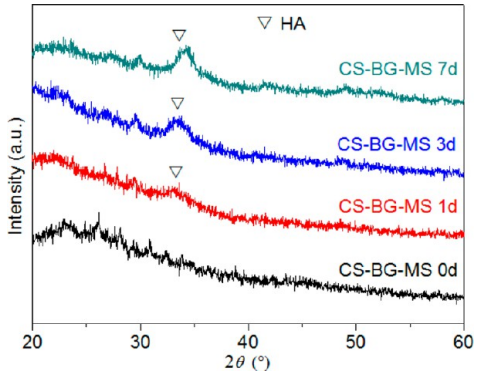

Figure 3. XRD spectra of CS-BG-MS membranes before and after immersion in SBF showing HA formation.

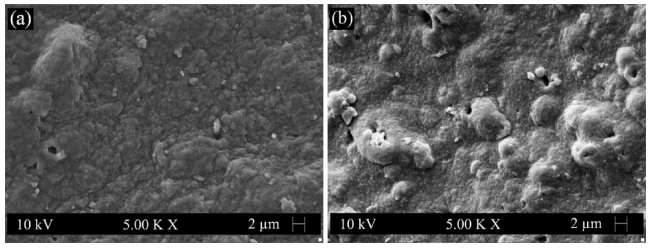

Figure 5. SEM images of (a) CS-BG membranes and (b) CS-BG-MS membranes after immersion in SBF for 7 days.

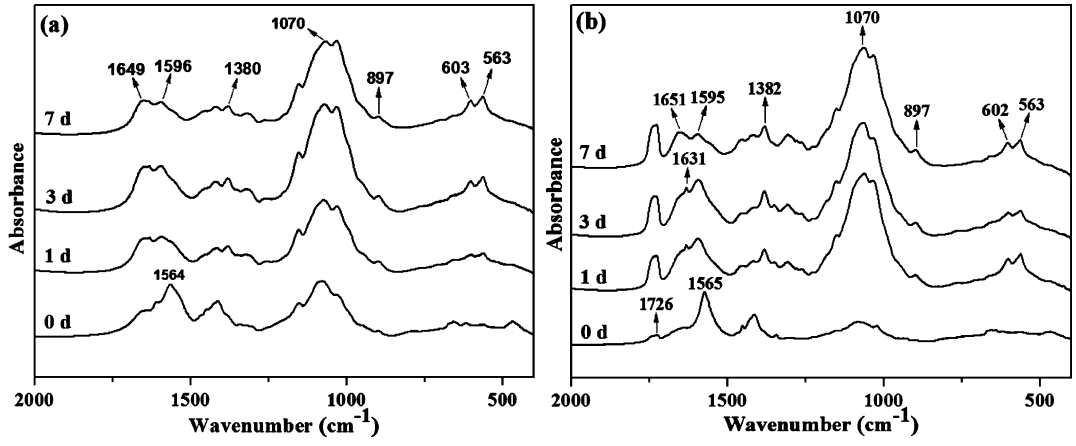

Figure 4. FTIR spectra of (a) CS-BG membranes and (b) CS-BG-MS membranes before and after immersion in SBF. (The peaks of relevance are discussed in the text.)

DOI: 10.1021/acsami.5b06128
ACS Appl. Mater. Interfaces 2015, 7, 20845−20854

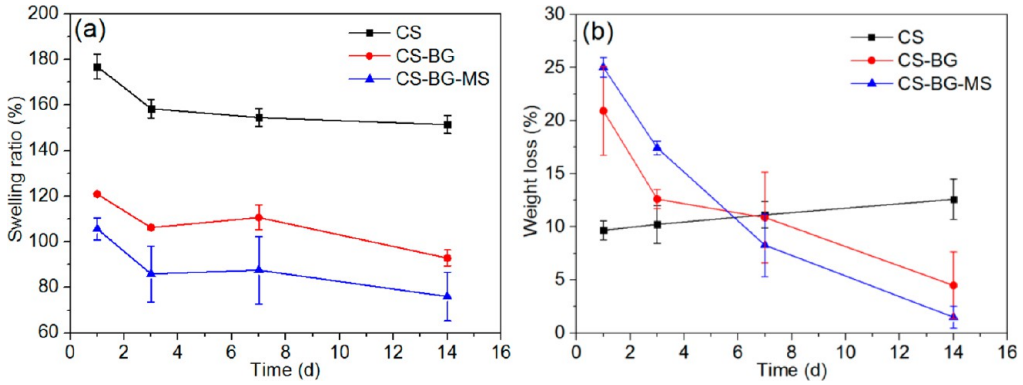

Figure 6. (a) Swelling and (b) degradation behaviors of CS, CS-BG, and CS-BG-MS membranes in SBF.

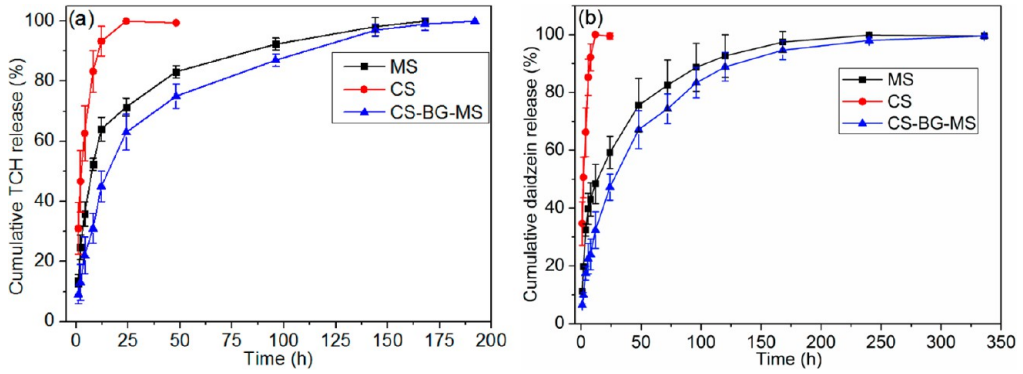

Figure 7. (a) TCH release behavior in PBS and (b) daidzein release behavior in PBS/ethanol from MS, CS, and CS-BG-MS membranes.

The superior bioactivity of the prepared composite membranes suggests that they have the potential ability to bond with bone tissue, which is advantageous for applications of GTR/GBR membranes.[3]

3.6. Swelling and Degradation. For GTR/GBR membranes, the swelling ratio must be studied because the membranes will eventually be surrounded by blood and body fluids during surgical placement.[6] A high swelling ratio may not be favorable not only because the space occupied by the GTR/GBR membranes is limited but also because higher water uptake may possibly allow a greater infiltration of cells.[9] The pure CS membranes exhibited a relatively higher swelling capacity in a period of 14 days, and the incorporation of BG and MS decreased the swelling ratio gradually (Figure 6a). This behavior may be due to the decrease of CS content (wt %) in the CS-BG and CS-BG-MS membranes and the incorporated BG as well as MS; however, they do not significantly absorb water like CS does. A reduction in water uptake was also found in other studies upon addition of bioactive glass/ceramic particles to CS membranes or scaffolds.[9,39]

The controlled degradation of GTR/GBR membranes is important to avoid the removal of membranes by a second surgical procedure and to provide space for newly formed tissues. According to Figure 6b, the weight loss of the CS membranes increased gradually, while that of both CS-BG and CS-BG-MS membranes decreased after 1 day of SBF immersion. During immersion in SBF, two processes take place, namely, the degradation of membranes and the formation of HA on the membranes surfaces. The results of the *in vitro* bioactivity test demonstrated that HA began to form on the CS-BG and CS-BG-MS membranes after 1 day of SBF immersion. Therefore, it is likely that the HA formation rate was higher than the degradation rate of the composite membranes after 1 day, which leads to the reduced weight loss of the CS-BG and CS-BG-MS membranes. The slow degradation rate of the CS-BG and CS-BG-MS membranes at the early stage of immersion in SBF suggests that these membranes have the potential to avoid collapse and perform their barrier function.

3.7. Drug Release. Figure 7a shows the cumulative percentage of TCH released from MS, CS, and CS-BG-MS membranes, while Figure 7b shows the daidzein release profiles. All samples showed an initial burst release of TCH or daidzein, in which the highest one was observed for CS membranes and the lowest one was for CS-BG-MS membranes. The TCH directly loaded in the CS membranes was completely released within 24 h, while the TCH release was found to be more sustained in the MS and CS-BG-MS membranes over a period of ~7 days. Daidzein loaded CS membranes exhibited a short release period of 12 h. In contrast, MS and CS-BG-MS membranes sustainably released the daidzein for ~10 days. Such release profiles demonstrate that the encapsulation of TCH or daidzein in MS was effective in reducing the initial burst release and prolonging the release time. It was interesting to note that the release rate of TCH or daidzein in the MS was higher than that in the CS-BG-MS membranes during the initial stage of release. This may be due to the fact that most of the MS were embedded in the CS matrix (Figure 2d); therefore, the CS matrix acts as a barrier for TCH or daidzein release from the MS. A similar delayed release phenomenon has been observed in a previous study.[40]

As discussed elsewhere,[17] vancomycin release from PHBV microspheres was mainly diffusion controlled due to the high solubility of vancomycin and slow degradation rate of PHBV in

DOI: 10.1021/acsami.5b06128
ACS Appl. Mater. Interfaces 2015, 7, 20845−20854

the release media. Both TCH and daidzein readily dissolve in their corresponding release medium, and the degradation as well as swelling of PHBV in PBS or PBS/ethanol solution were negligible during the release period (data not shown). Therefore, TCH or daidzein release from PHBV microspheres is likely to be mainly controlled by diffusion. In order to verify this assumption, the drug release data of MS and CS-BG-MS membranes were analyzed using the Higuchi equation which has been widely used to describe diffusion controlled drug release behavior.[29] Good linear correlations ($R^2 \geq 0.968$) were obtained for all samples (Figure S5a), indicating the TCH or daidzein release from MS and CS-BG-MS membranes is controlled by diffusion. Since CS will swell upon immersion in aqueous solution, the drug release data of CS-BG-MS membranes was further analyzed by Peppas equation in which the influence of swelling is taken into consideration.[28] The obtained linear correlations ($R^2 \geq 0.993$, Figure S5b) were higher compared to the fitting using the Higuchi equation. The release exponents were 0.63 and 0.61 for TCH and daidzein loaded CS-BG-MS membranes, respectively, which indicates that the CS-BG-MS membranes exhibited an anomalous drug transport behavior.[41] If compared to the characteristic release exponent of Fickian diffusion ($n = 0.5$) and Case-II transport ($n = 1.0$), the release exponent of CS-BG-MS membranes ($n = 0.63$ or 0.61) is found to be relatively closer to Fickian diffusion rather than Case-II transport, suggesting that the TCH or daidzein release from the CS-BG-MS membranes is mainly dependent on diffusion.

The delivery of multiple therapeutic drugs is highly beneficial to induce the complete regeneration of periodontal tissues, which, however, has not yet attracted sufficient attention in developing GTR/GBR membranes.[42] Bacterial infection and osteoporosis are two important factors leading to delayed or failed periodontal regeneration.[8,21−23] Therefore, it is of significance to endow the GTR/GBR membranes with the ability to deliver both antibacterial and antiosteoporosis drugs. In the present study, a sustained and controlled TCH (antibiotic) and daidzein (antiosteoporosis drug) release function can be effectively imparted to the CS-BG-MS membranes using TCH or daidzein loaded MS. Moreover, TCH and daidzein possess completely different hydrophilic/hydrophobic properties. Therefore, the developed CS-BG-MS membranes can be considered to have high potential for the local delivery of multiple drugs using microspheres loaded with different drugs.

3.8. Cytotoxicity and Live/Dead Assay. MG-63 cells have been widely used to preliminary evaluate the biocompatibility of biomaterials for supporting osteogenic growth.[9,43,44] Cytotoxicity of the CS, CS-BG, and CS-BG-MS membranes toward MG-63 cells is shown in Figure 8. Cells cultured in the absence of membranes were taken as the control. On day 1, the cell viability was not significantly different among the control and the three types of membranes, indicating similar cell viability. On day 2, a significant difference in cell viability was observed between the control and CS-BG membranes ($P < 0.001$) as well as between the control and CS-BG-MS membranes ($P < 0.01$). In addition, no statistical difference was found between the CS-BG and CS-BG-MS membranes. The presence of cells on the CS, CS-BG, and CS-BG-MS membranes was also evaluated using a Live/Dead assay (Figure 9). On day 1, fluorescence microscope micrographs showed more live cells on the CS-BG membranes (Figure 9c) than on the CS membranes (Figure 9a) and CS-BG-MS membranes

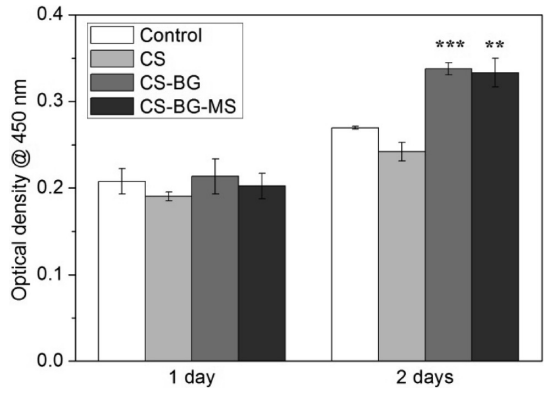

Figure 8. Cell viability of MG-63 cells cultured on CS, CS-BG, and CS-BG-MS membranes for 1 and 2 days (**$P < 0.01$, ***$P < 0.001$).

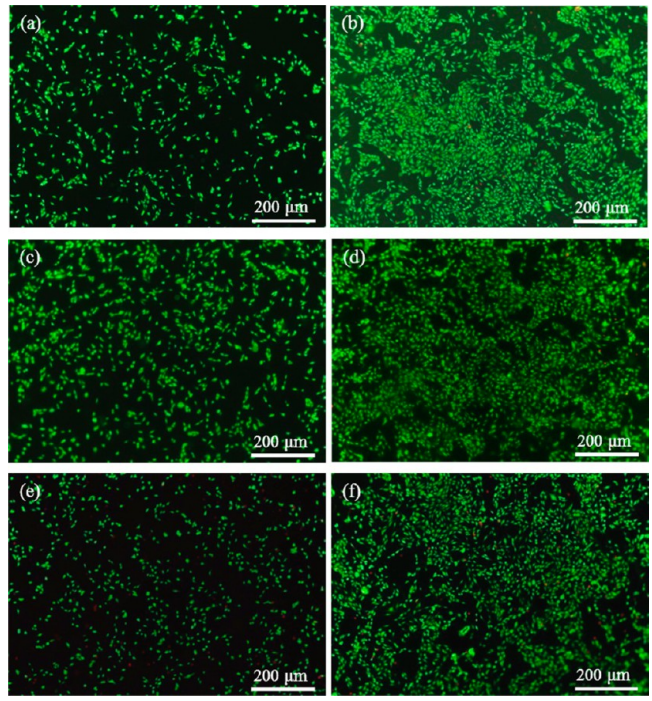

Figure 9. Live (green)/Dead (red) assay of MG-63 cells cultured on: (a,b) CS membranes, (c,d) CS-BG membranes, and (e,f) CS-BG-MS membranes for 1 day (left column) and 4 days (right column).

(Figure 9e), which is consistent with the CCK8 results (Figure 8). After 4 days of cultivation, MG-63 cells proliferated in all three types of membranes, and the CS-BG membranes (Figure 9d) exhibited relatively more live cells. These results demonstrate that the presence of 45S5 BG promoted the proliferation of MG-63 cells, while the incorporation of MS has no significant effect on cell viability.

3.9. Cell Skeleton and Morphology. After 1 day of cultivation, cell phenotype on the extracts of CS membranes was comparatively round (Figure 10a), while cells on the extracts of CS-BG and CS-BG-MS membranes showed elongated filopodia (Figure 10c,e). On day 4, cells were grouped on the CS-BG sample, and well-organized fibrous F-actin was observed on the CS, CS-BG, and CS-BG-MS samples. Cell filopodia extension is dependent on the substrate properties. These results suggest that CS do not favor cell spreading on day 1, while the cell spreading was better on day 4. Furthermore, the addition of 45S5 BG has a positive

DOI: 10.1021/acsami.5b06128
ACS Appl. Mater. Interfaces 2015, 7, 20845−20854

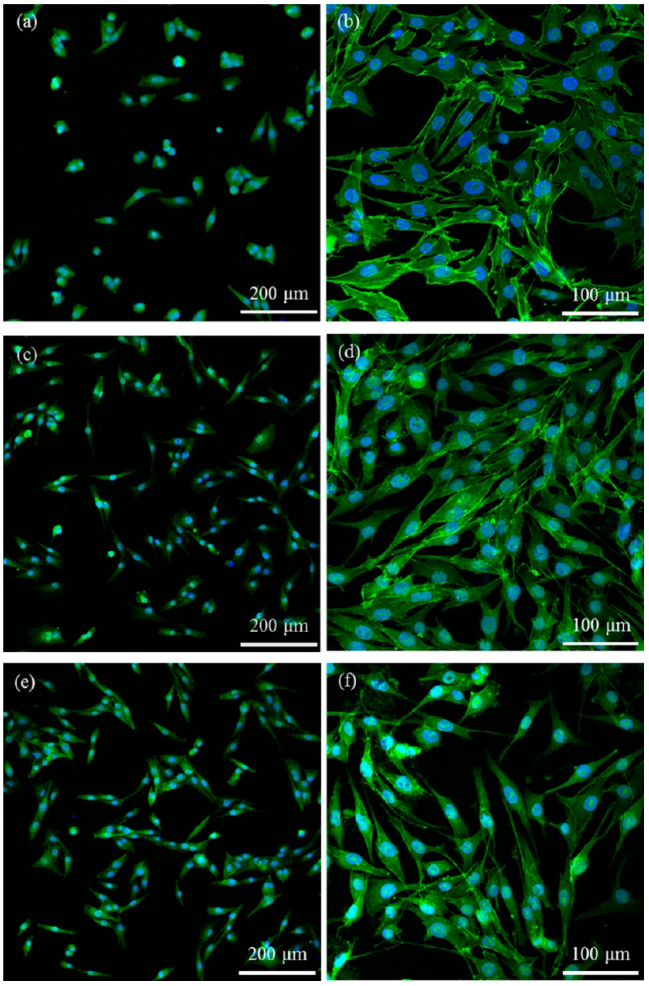

Figure 10. Fluorescence images of cell skeletons of MG-63 cells grown on the extracts of: (a,b) CS membranes, (c,d) CS-BG membranes, and (e,f) CS-BG-MS membranes for 1 day (left column) and 4 days (right column).

influence on the F-actin cytoskeletal organization after 4 days of cultivation.

The morphologies of MG-63 cells on the CS, CS-BG, and CS-BG-MS membranes are shown in Figure 11. After 1 day of cultivation, the cells adhered on the surface of the CS-BG and CS-BG-MS membranes with cells exhibiting more expressed filopodia in CS-BG-MS membranes than on CS membranes, indicating that 45S5 BG significantly promotes the adhesion of MG-63 cells. The addition of 45S5 BG induced increased surface roughness on the membranes that might help the anchorage and attachment of the cells to the surface.[30,45]

3.10. Alkaline Phosphatase Activity. ALP is a common marker of early interim osteoblast activity. ALP activity was measured at 7 and 14 days on the CS, CS-BG, and CS-BG-MS membranes (Figure 12). Cells cultured without the presence of membranes were chosen as control. In a culture period of 7 days, no significant differences were observed between the control and the three types of membranes. However, MG-63 cells expressed higher ALP activities on the CS-BG and CS-BG-MS membranes ($P < 0.001$) after 14 days of cultivation, while the difference between the control and CS membranes was still not significantly different. All results above demonstrate that CS has no obvious effect on the activity of MG-63 cells, while 45S5 BG can significantly increase the activity of MG-63 cells with

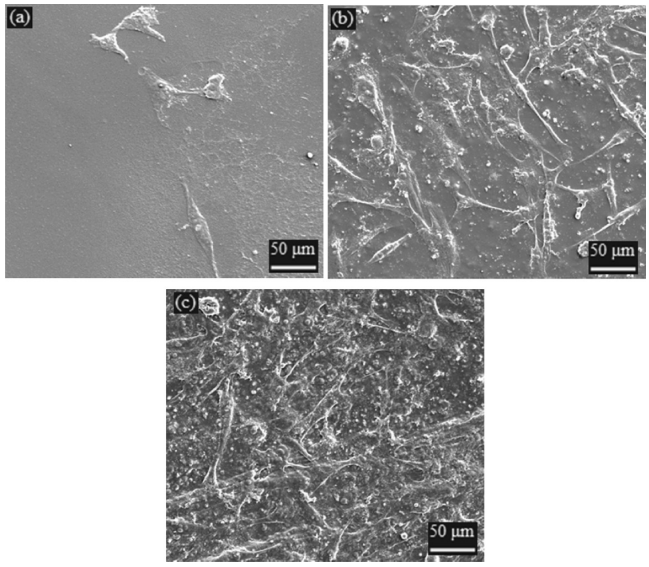

Figure 11. SEM images of MG-63 cells cultured on (a) CS membranes, (b) CS-BG membranes, and (c) CS-BG-MS membranes after 1 day of cultivation.

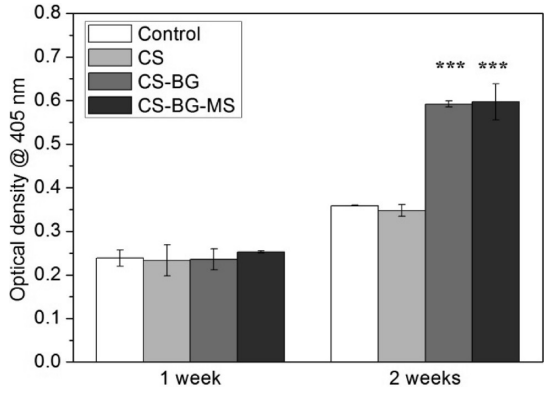

Figure 12. ALP activity of MG-63 cells on CS, CS-BG, and CS-BG-MS membranes after 1 and 2 weeks of cultivation.

the extension of cultivation time. A similar effect of BG on MG-63 cell activity is also reported in the literature.[45,46] For example, the ALP activity was enhanced when MG-63 cells were grown on P(3HB) films incorporated with 45S5 BG nanoparticles.[45] The enhanced ALP activity of bioactive glass/polymer composites compared to the pure polymer may be related to the release of ions from the bioactive glass contained in the composites known to induce osteoblast differentiation.[45]

The above cell biology studies demonstrate that osteoblast-like MG-63 cells can attach, spread, and proliferate on the developed CS-BG and CS-BG-MS membranes, showing the potential of such composite membranes to support new bone formation, which is an important preliminary step to allow PDL anchorage and growth.[9]

4. CONCLUSIONS

CS, CS-BG, and CS-BG-MS membranes intended for GTR/GBR were prepared by the solution casting method. The introduction of 45S5 BG particles and PHBV microspheres into CS increased the roughness, hydrophilicity, and flexibility while decreasing the swelling ratio and degradation rate of the membranes. All membranes showed slow degradation at the

DOI: 10.1021/acsami.5b06128
ACS Appl. Mater. Interfaces 2015, 7, 20845−20854

early stage of immersion in SBF. HCA began to form on CS-BG and CS-BG-MS membranes after immersion in SBF for 1 day, indicating a superior bioactivity. PHBV microspheres were used as drug carriers in the CS-BG-MS membranes. Compared to the CS membranes, CS-BG-MS membranes exhibited a more sustained and controlled release of TCH and daidzein. *In vitro* cell tests revealed that the CS-BG and CS-BG-MS membranes induced higher cell adhesion and cell viability compared to CS membranes. Furthermore, the incorporation of 45S5 BG particles into CS membranes significantly promoted ALP activity, which confirmed the osteoconductive character of the CS-BG and CS-BG-MS membranes. The developed multifunctional CS-BG-MS membranes are thus a promising polymer/bioactive glass composite system for GTR/GBR applications, and future studies should consider other cell types (e.g., PDL fibroblasts) before *in vivo* testing using GTR/GBR periodontal defect models.

■ ASSOCIATED CONTENT

Supporting Information

The Supporting Information is available free of charge on the ACS Publications website at DOI: 10.1021/acsami.5b06128.

EDS results, typical stress−strain curves of tensile test, and fitting results of drug release data (PDF)

■ AUTHOR INFORMATION

Corresponding Authors

*E-mail: yaoqing400@163.com (Q.Y.).
*E-mail: aldo.boccaccini@ww.uni-erlangen.de. Tel.: +49 9131 85 28601. Fax: +49 9131 85 28602 (A.R.B.).

Notes

The authors declare no competing financial interest.

■ ACKNOWLEDGMENTS

The authors thank Jennifer Reiser (Institute of Polymer Materials, FAU) for the roughness measurement and Florian Niekiel (Institute of Micro- and Nanostructure Research, FAU) for sputter coating. W.L. (No. 2011628002) and Y.D. (No. 2011628003) would like to acknowledge the China Scholarship Council (CSC) for financial support. Q.Y. is grateful for financial support from the Zhejiang National Nature Science Foundation (LQ15H180003).

■ REFERENCES

(1) Wang, H. L.; Greenwell, H.; Fiorellini, J.; Giannobile, W.; Offenbacher, S.; Salkin, L.; Townsend, C.; Sheridan, P.; Genco, R. J. Periodontal Regeneration. *J. Periodontol.* **2005**, *76*, 1601−1622.

(2) Mota, J.; Yu, N.; Caridade, S. G.; Luz, G. M.; Gomes, M. E.; Reis, R. L.; Jansen, J. A.; Walboomers, X. F.; Mano, J. F. Chitosan/Bioactive Glass Nanoparticle Composite Membranes for Periodontal Regeneration. *Acta Biomater.* **2012**, *8*, 4173−80.

(3) Bottino, M. C.; Thomas, V.; Schmidt, G.; Vohra, Y. K.; Chu, T.-M. G.; Kowolik, M. J.; Janowski, G. M. Recent Advances in the Development of GTR/GBR Membranes for Periodontal Regeneration—A Materials Perspective. *Dent. Mater.* **2012**, *28*, 703−721.

(4) Rowe, M. J.; Kamocki, K.; Pankajakshan, D.; Li, D.; Bruzzaniti, A.; Thomas, V.; Blanchard, S. B.; Bottino, M. C. Dimensionally Stable and Bioactive Membrane for Guided Bone Regeneration: An *In Vitro* Study. *J. Biomed. Mater. Res., Part B* **2015**, DOI: 10.1002/jbm.b.33430.

(5) Xu, C.; Lei, C.; Meng, L.; Wang, C.; Song, Y. Chitosan as a Barrier Membrane Material in Periodontal Tissue Regeneration. *J. Biomed. Mater. Res., Part B* **2012**, *100B*, 1435−1443.

(6) Gentile, P.; Chiono, V.; Tonda - Turo, C.; Ferreira, A. M.; Ciardelli, G. Polymeric Membranes for Guided Bone Regeneration. *Biotechnol. J.* **2011**, *6*, 1187−1197.

(7) Leal, A. I.; Caridade, S. G.; Ma, J.; Yu, N.; Gomes, M. E.; Reis, R. L.; Jansen, J. A.; Walboomers, X. F.; Mano, J. F. Asymmetric PDLLA Membranes Containing Bioglass® for Guided Tissue Regeneration: Characterization and *In Vitro* Biological Behavior. *Dent. Mater.* **2013**, *29*, 427−436.

(8) Xue, J.; He, M.; Liu, H.; Niu, Y.; Crawford, A.; Coates, P. D.; Chen, D.; Shi, R.; Zhang, L. Drug Loaded Homogeneous Electrospun PCL/Gelatin Hybrid Nanofiber Structures for Anti-Infective Tissue Regeneration Membranes. *Biomaterials* **2014**, *35*, 9395−9405.

(9) Qasim, S. B.; Delaine-Smith, R. M.; Fey, T.; Rawlinson, A.; Rehman, I. U. Freeze Gelated Porous Membranes for Periodontal Tissue Regeneration. *Acta Biomater.* **2015**, *23*, 317.

(10) Zhao, X.; Wu, y.; Du, Y.; Chen, X.; Lei, B.; Xue, Y.; Ma, P. X. A Highly Bioactive and Biodegradable Poly (Glycerol Sebacate)-Silica Glass Hybrid Elastomer with Tailored Mechanical Properties for Bone Tissue Regeneration. *J. Mater. Chem. B* **2015**, *3*, 3222−3233.

(11) Jones, J. R. Review of Bioactive Glass: From Hench to Hybrids. *Acta Biomater.* **2013**, *9*, 4457−4486.

(12) Gorustovich, A. A.; Roether, J. A.; Boccaccini, A. R. Effect of Bioactive Glasses on Angiogenesis: A Review of *In Vitro* and *In Vivo* Evidences. *Tissue Eng., Part B* **2010**, *16*, 199−207.

(13) Hench, L. L. Opening Paper 2015-Some Comments on Bioglass: Four Eras of Discovery and Development. *Biomedical glasses* **2015**, *1*, 1−11.

(14) Miguez-Pacheco, V.; Hench, L. L.; Boccaccini, A. R. Bioactive Glasses beyond Bone and Teeth: Emerging Applications in Contact with Soft Tissues. *Acta Biomater.* **2015**, *13*, 1−15.

(15) He, J.; Zhu, X.; Qi, Z.; Wang, C.; Mao, X.; Zhu, C.; He, Z.; Li, M.; Tang, Z. Killing Dental Pathogens Using Antibacterial Graphene Oxide. *ACS Appl. Mater. Interfaces* **2015**, *7*, 5605−5611.

(16) Li, M.; Rouaud, O.; Poncelet, D. Microencapsulation by Solvent Evaporation: State of the Art for Process Engineering Approaches. *Int. J. Pharm.* **2008**, *363*, 26−39.

(17) Li, W.; Ding, Y.; Rai, R.; Roether, J. A.; Schubert, D. W.; Boccaccini, A. R. Preparation and Characterization of PHBV Microsphere/45S5 Bioactive Glass Composite Scaffolds with Vancomycin Releasing Function. *Mater. Sci. Eng., C* **2014**, *41*, 320−328.

(18) Li, W.; Nooeaid, P.; Roether, J. A.; Schubert, D. W.; Boccaccini, A. R. Preparation and Characterization of Vancomycin Releasing PHBV Coated 45S5 Bioglass®-Based Glass−Ceramic Scaffolds for Bone Tissue Engineering. *J. Eur. Ceram. Soc.* **2014**, *34*, 505−514.

(19) Hazer, D. B.; Kılıçay, E.; Hazer, B. Poly(3-Hydroxyalkanoate)S: Diversification and Biomedical Applications: A State of the Art Review. *Mater. Sci. Eng., C* **2012**, *32*, 637−647.

(20) Köse, G. T.; Kenar, H.; Hasırcı, N.; Hasırcı, V. Macroporous Poly(3-Hydroxybutyrate-Co-3-Hydroxyvalerate) Matrices for Bone Tissue Engineering. *Biomaterials* **2003**, *24*, 1949−1958.

(21) Gomes-Filho, I. S.; Passos, J. d. S.; Cruz, S. S.; Vianna, M. I. P.; Cerqueira, E. d. M. M.; Oliveira, D. C.; dos Santos, C. A. S. T.; Coelho, J. M. F.; Sampaio, F. P.; Freitas, C. O. T.; de Oliveira, N. F. The Association between Postmenopausal Osteoporosis and Periodontal Disease. *J. Periodontol.* **2007**, *78*, 1731−1740.

(22) Passos, J. S.; Vianna, M. I. P.; Gomes-Filho, I. S.; Cruz, S. S.; Barreto, M. L.; Adan, L.; Rösing, C. K.; Cerqueira, E. M. M.; Trindade, S. C.; Coelho, J. M. F. Osteoporosis/Osteopenia as an Independent Factor Associated with Periodontitis in Postmenopausal Women: A Case−Control Study. *Osteoporosis Int.* **2013**, *24*, 1275−1283.

(23) Lin, T.-H.; Lung, C.-C.; Su, H.-P.; Huang, J.-Y.; Ko, P.-C.; Jan, S.-R.; Sun, Y.-H.; Nfor, O. N.; Tu, H.-P.; Chang, C.-S.; Jian, Z.-H.; Chiang, Y.-C.; Liaw, Y.-P. Association between Periodontal Disease and Osteoporosis by Gender: A Nationwide Population-Based Cohort Study. *Medicine* **2015**, *94*, e553.

(24) Arcos, D.; Boccaccini, A. R.; Bohner, M.; Díez-Pérez, A.; Epple, M.; Gómez-Barrena, E.; Herrera, A.; Planell, J. A.; Rodríguez-Mañas,

L.; Vallet-Regí, M. The Relevance of Biomaterials to the Prevention and Treatment of Osteoporosis. *Acta Biomater.* **2014**, *10*, 1793−1805.
(25) Zhang, Z.; Huang, Y.; Gao, F.; Bu, H.; Gu, W.; Li, Y. Daidzein-Phospholipid Complex Loaded Lipid Nanocarriers Improved Oral Absorption: *In Vitro* Characteristics and *In Vivo* Behavior in Rats. *Nanoscale* **2011**, *3*, 1780−1787.
(26) Kokubo, T.; Takadama, H. How Useful Is SBF in Predicting *In Vivo* Bone Bioactivity? *Biomaterials* **2006**, *27*, 2907−2915.
(27) Scheithauer, E. C.; Li, W.; Ding, Y.; Harhaus, L.; Roether, J. A.; Boccaccini, A. R. Preparation and Characterization of Electrosprayed Daidzein-Loaded PHBV Microspheres. *Mater. Lett.* **2015**, *158*, 66−69.
(28) Ritger, P. L.; Peppas, N. A. A Simple Equation for Description of Solute Release II. Fickian and Anomalous Release from Swellable Devices. *J. Controlled Release* **1987**, *5*, 37−42.
(29) Higuchi, T. Rate of Release of Medicaments from Ointment Bases Containing Drugs in Suspension. *J. Pharm. Sci.* **1961**, *50*, 874−5.
(30) Costa, D. O.; Prowse, P. D. H.; Chrones, T.; Sims, S. M.; Hamilton, D. W.; Rizkalla, A. S.; Dixon, S. J. The Differential Regulation of Osteoblast and Osteoclast Activity by Surface Topography of Hydroxyapatite Coatings. *Biomaterials* **2013**, *34*, 7215−7226.
(31) Fu, S.-Y.; Feng, X.-Q.; Lauke, B.; Mai, Y.-W. Effects of Particle Size, Particle/Matrix Interface Adhesion and Particle Loading on Mechanical Properties of Particulate-Polymer Composites. *Composites, Part B* **2008**, *39*, 933−961.
(32) Boyan, B. D.; Hummert, T. W.; Dean, D. D.; Schwartz, Z. Role of Material Surfaces in Regulating Bone and Cartilage Cell Response. *Biomaterials* **1996**, *17*, 137−146.
(33) Bretcanu, O.; Misra, S.; Roy, I.; Renghini, C.; Fiori, F.; Boccaccini, A. R.; Salih, V. *In Vitro* Biocompatibility of 45S5 Bioglass®-Derived Glass-Ceramic Scaffolds Coated with Poly(3-Hydroxybutyrate). *J. Tissue Eng. Regener. Med.* **2009**, *3*, 139−148.
(34) Wenzel, R. N. Resistance of Solid Surfaces to Wetting by Water. *Ind. Eng. Chem.* **1936**, *28*, 988−994.
(35) Li, W.; Garmendia, N.; Perez de Larraya, U.; Ding, Y.; Detsch, R.; Gruenewald, A.; Roether, J.; Schubert, D.; Boccaccini, A. R. 45S5 Bioactive Glass-Based Scaffolds Coated with Cellulose Nanowhiskers for Bone Tissue Engineering. *RSC Adv.* **2014**, *4*, 56156−56164.
(36) Groh, D.; Döhler, F.; Brauer, D. S. Bioactive Glasses with Improved Processing. Part 1. Thermal Properties, Ion Release and Apatite Formation. *Acta Biomater.* **2014**, *10*, 4465−4473.
(37) Enescu, D.; Hamciuc, V.; Ardeleanu, R.; Cristea, M.; Ioanid, A.; Harabagiu, V.; Simionescu, B. C. Polydimethylsiloxane Modified Chitosan. Part III: Preparation and Characterization of Hybrid Membranes. *Carbohydr. Polym.* **2009**, *76*, 268−278.
(38) Lawrie, G.; Keen, I.; Drew, B.; Chandler-Temple, A.; Rintoul, L.; Fredericks, P.; Grøndahl, L. Interactions between Alginate and Chitosan Biopolymers Characterized Using FTIR and XPS. *Biomacromolecules* **2007**, *8*, 2533−2541.
(39) Peter, M.; Binulal, N. S.; Soumya, S.; Nair, S. V.; Furuike, T.; Tamura, H.; Jayakumar, R. Nanocomposite Scaffolds of Bioactive Glass Ceramic Nanoparticles Disseminated Chitosan Matrix for Tissue Engineering Applications. *Carbohydr. Polym.* **2010**, *79*, 284−289.
(40) Paris, J. L.; Román, J.; Manzano, M.; Cabañas, M. V.; Vallet-Regí, M. Tuning Dual-Drug Release from Composite Scaffolds for Bone Regeneration. *Int. J. Pharm.* **2015**, *486*, 30−37.
(41) Siepmann, J.; Peppas, N. A. Higuchi Equation: Derivation, Applications, Use and Misuse. *Int. J. Pharm.* **2011**, *418*, 6−12.
(42) Chen, F.-M.; An, Y.; Zhang, R.; Zhang, M. New Insights into and Novel Applications of Release Technology for Periodontal Reconstructive Therapies. *J. Controlled Release* **2011**, *149*, 92−110.
(43) Li, W.; Wang, H.; Ding, Y.; Scheithauer, E. C.; Goudouri, O.-M.; Grünewald, A.; Detsch, R.; Agarwal, S.; Boccaccini, A. R. Antibacterial 45S5 Bioglass®-Based Scaffolds Reinforced with Genipin Cross-Linked Gelatin for Bone Tissue Engineering. *J. Mater. Chem. B* **2015**, *3*, 3367−3378.
(44) Pishbin, F.; Mourino, V.; Flor, S.; Kreppel, S.; Salih, V.; Ryan, M. P.; Boccaccini, A. R. Electrophoretic Deposition of Gentamicin-Loaded Bioactive Glass/Chitosan Composite Coatings for Orthopaedic Implants. *ACS Appl. Mater. Interfaces* **2014**, *6*, 8796−8806.
(45) Misra, S. K.; Ansari, T.; Mohn, D.; Valappil, S. P.; Brunner, T. J.; Stark, W. J.; Roy, I.; Knowles, J. C.; Sibbons, P. D.; Jones, E. V.; Boccaccini, A. R.; Salih, V. Effect of Nanoparticulate Bioactive Glass Particles on Bioactivity and Cytocompatibility of Poly(3-Hydroxybutyrate) Composites. *J. R. Soc., Interface* **2010**, *7*, 453−465.
(46) Sola, A.; Bellucci, D.; Raucci, M. G.; Zeppetelli, S.; Ambrosio, L.; Cannillo, V. Heat Treatment of Na_2O-CaO-P_2O_5-SiO_2 Bioactive Glasses: Densification Processes and Postsintering Bioactivity. *J. Biomed. Mater. Res., Part A* **2012**, *100A*, 305−322.

DOI: 10.1021/acsami.5b06128
ACS Appl. Mater. Interfaces 2015, 7, 20845−20854